



Magnetic polarons in $\text{Ca}_{1-x}\text{Y}_x\text{MnO}_3$

H. Aliaga*, M.T. Causa, M. Tovar, B. Alascio

Comisión Nacional de Energía Atómica, Centro Atómico Bariloche and Instituto Balseiro, 8400 S.C. de Bariloche, Argentina

Abstract

Experimental evidence shows that in the magnetoresistive manganite $\text{Ca}_{1-x}\text{Y}_x\text{MnO}_3$, ferromagnetic (FM) polarons arises in an antiferromagnetic (AF) background, as a result of the doping with yttrium. This hypothesis is supported in this work by classical Monte Carlo calculations performed on a model where FM double exchange and AF superexchange compete. © 2002 Elsevier Science B.V. All rights reserved.

Keywords: Manganites; Double exchange; Magnetoresistance; Magnetic polarons

In this work, we try to explain experimental results [1,2] on magnetoresistive $\text{Ca}_{1-x}\text{Y}_x\text{MnO}_3$ doped manganites, that point towards the existence of magnetic polarons. The pure sample ($x = 0$) presents G-type antiferromagnetic (AF) ordering with a transition temperature $T_N = 123$ K, and insulator characteristics. In this sample, all the Mn ions have valence $4+$, where the localized t_{2g} spins have a spin $S = \frac{3}{2}$. As yttrium ions are added, itinerant e_g electrons with spin $s = \frac{1}{2}$ are introduced and there is a mixed valence state of Mn^{4+} and Mn^{3+} in the proportion $(1 - x)$ and x , respectively. The magnetic moment raises [1] and the resistivity drops sharply as x is increased up to $x \leq 0.15$. A thermally activated polaronic behavior for the conductivity was fitted between room temperature and 100 K. The experimental results were interpreted in terms of ferromagnetic (FM) polarons, produced by the alignment of neighboring t_{2g} spins by the e_g electrons and immersed in the AF background. In this work, we compare the experimental

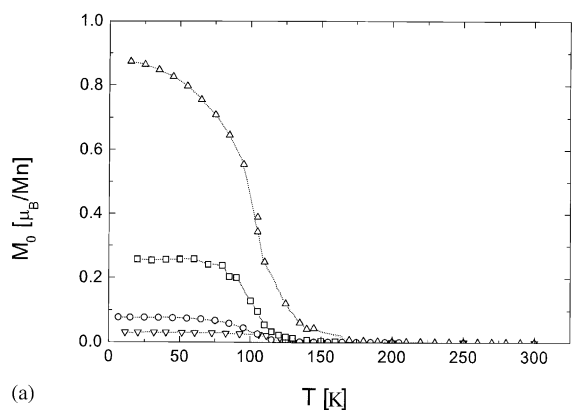
magnetic measurements with the properties predicted by Monte Carlo (MC) calculations on a model where FM–double exchange (FM–DE) and AF–superexchange (AF–SE) interactions compete.

Ceramic polycrystalline samples of $\text{Ca}_{1-x}\text{Y}_x\text{MnO}_3$ were prepared by solid-state reaction methods [3]. Room temperature X-rays diffractograms show that all the samples crystallize in an orthorhombic Pnma cell. The DC magnetization, M , was measured with a SQUID magnetometer between 5 and 300 K for $H \leq 50$ kOe.

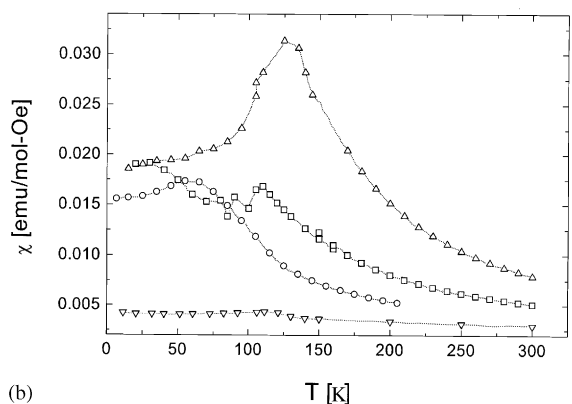
We measured M vs. H at different temperatures for the samples $x = 0, 0.03, 0.05$ and 0.1 and we found a linear dependence at high fields: $M = M_0 + \chi H$. In Fig. 1(a) we show M_0 vs. T . The behavior resembles that of a ferromagnet with a characteristic ordering temperature T_{mo} , almost constant for all the samples. For $x = 0$, a small $M_0 \sim 0.03\mu_B/\text{f.u.}$ reflects a weak ferromagnetic Dzialoshinskii–Moriya interaction [1]. In Fig. 2(a) we plot M_0 vs. x at $T = 5$ K. The curve has an S shape starting with a slope of $1\mu_B$ per Mn^{3+} ion and reaching a slope $M_0/x \sim 7\mu_B$ at $x = 0.07$. Notice that full FM alignment ($3\mu_B/\text{Mn site}$) is not reached.

*Corresponding author. Fax: +54-2944-445299.

E-mail address: aliagah@cab.cnea.gov.ar (H. Aliaga).



(a)



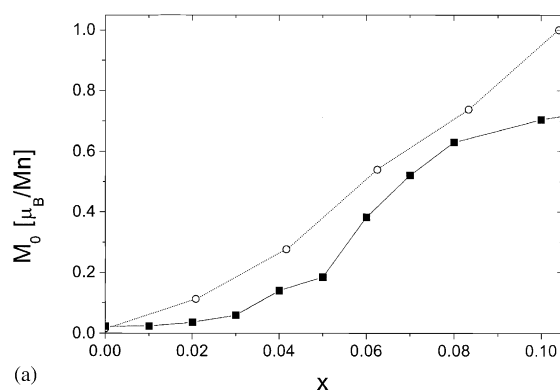
(b)

Fig. 1. (a) M_0 vs. T and (b) χ vs. T , for the samples $x = 0$ (down triangles), 0.03 (circles), 0.05 (squares), and 0.1 (up triangles).

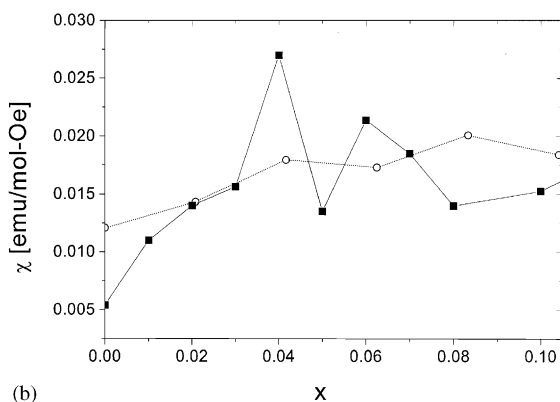
In Fig. 1(b), we show $\chi(T)$ vs. T . The general behavior above T_{mo} has been studied in Ref. [1], for $x = 0, 0.05, 0.07$ and 0.1. The most peculiar feature observed is a deviation from the Curie–Weiss law, presenting a negative curvature in $\chi^{-1}(T)$. This temperature dependence was described in terms of two contributions

$$\chi(T) = (1 - x)\chi_{\text{AF}}(T) + x\chi_{\text{FM}}(T), \quad (1)$$

where $\chi_{\text{AF}}(T)$ is the susceptibility of the AF background and $\chi_{\text{FM}}(T)$ reflects the strong FM–DE correlations that results in polaron formation in the PM phase. For $x = 0$, a maximum in $\chi(T)$ is present at T_{N} . For $x = 0.1$ the behavior is qualitatively similar: a maximum is observed around T_{mo} , although with a much larger value. Below T_{mo} , $\chi(T)$ decreases rapidly and reaches $\sim 0.6\chi(T_{\text{mo}})$ at $T = 5$ K. For the intermediate



(a)



(b)

Fig. 2. (a) M_0 and (b) χ , as function of doping x , measured at 5 K (squares), and calculated (circles).

concentration, $x = 0.05$, a peak at T_{mo} is only a relative maximum: $\chi(T)$ increases again below $T \sim 70$ K and $\chi_{\text{AF}}(5\text{K}) \sim 1.2\chi(T_{\text{mo}})$. For the low-doped $x = 0.03$ sample no peak is observed at T_{mo} and $\chi(T)$ continues to increase below T_{mo} up to $T \sim 60$ K, where a broad maximum is present. The large values of $\chi(T_{\text{mo}})$ take into account the progressive polaron formation, indicated by the proportionality $\chi(T_{\text{mo}}) \propto x$, given by Eq. (1), where $\chi_{\text{AF}}(T_{\text{mo}}) \ll \chi_{\text{FM}}(T_{\text{mo}})$. In Fig. 2(b), we show $\chi(5\text{K})$ vs. x .

The simplest picture for the behavior of $M(H, T)$ below T_{mo} , is to associate $\chi(T)$ with the AF background and assume that $M_0(T)$ corresponds to the FM order of polarons. However, the measured $\chi(T)$ is in all cases much larger than the CaMnO_3 susceptibility. Thus, this simple model seems not appropriate to describe the experiments

in the ordered region. In order to obtain a better description of the magnetization behavior, we have performed a calculation of M vs. H using the numerical classical MC technique.

We consider the following Hamiltonian:

$$\mathcal{H} = - \sum_{\langle ij \rangle \sigma} t_{ij} (c_{i\sigma}^\dagger c_{j\sigma} + \text{h.c.}) - J_H \sum_i \mathbf{s}_i \cdot \mathbf{S}_i + g\mu_B H \sum_i S_{z,i} + K \sum_{\langle ij \rangle} \mathbf{S}_i \cdot \mathbf{S}_j. \quad (2)$$

Here $c_{i\sigma}^\dagger$ is the operator creating an itinerant electron of spin σ at site i , and $\mathbf{s}_i = \sum_{\alpha\beta} c_{i\alpha}^\dagger \boldsymbol{\sigma}_{\alpha\beta} c_{i\beta}$ gives the spin projection of the electron. Due to the strong Hund coupling ($J_H \rightarrow \infty$) between itinerant e_g electrons and the localized t_{2g} spins, only parallel spin projections were taken into account. In this way, the hopping of itinerant electrons depends on the orientation of the localized t_{2g} spins, according to the DE expression in one dimension: $t_{ij} = t \cos(\theta_{ij}/2)$, where θ_{ij} is the relative angle between localized spins \mathbf{S}_i and \mathbf{S}_j , t is the hopping parameter. The third term, represents Zeeman coupling between magnetic field H and $S_{z,i}$, the z component of localized spin \mathbf{S}_i . The AF–SE interaction between localized neighboring spins \mathbf{S}_i and \mathbf{S}_j is represented by the last term in Eq. (2). Numerical calculations were performed in one dimension, using the MC algorithm for a 48 sites chain with open boundary conditions. The localized spins were classical with modulus 1, and later renormalized to $(3+x)\mu_B$ in order to compare with experiments. Local changes in t_{2g} spins were made in conjunction with exact diagonalization of the itinerant electron system. The resulting electronic energy levels were then filled by the available number of electrons in the canonical ensemble. We take the hopping parameter $t = 0.1$ eV as the reference energy, and the temperature $T = 0.005t \sim 6$ K. Mermin–Wagner’s theorem precludes magnetic ordering at finite temperatures in 1D systems. However, we estimated a value for K from the ordering temperature T_{mo} that would arise from a classical Heisenberg model for a system with $z = 2$ neighbors. For $T_{\text{mo}} \sim 100$ K, we derive $KS^2/t = 0.05$.

In Fig. 3, we show M vs. H dependence for the 1D chain, when 0, 1, ..., 5 electrons are added (equivalent to dopings $x = 0, 0.02, \dots, 0.1$). For the

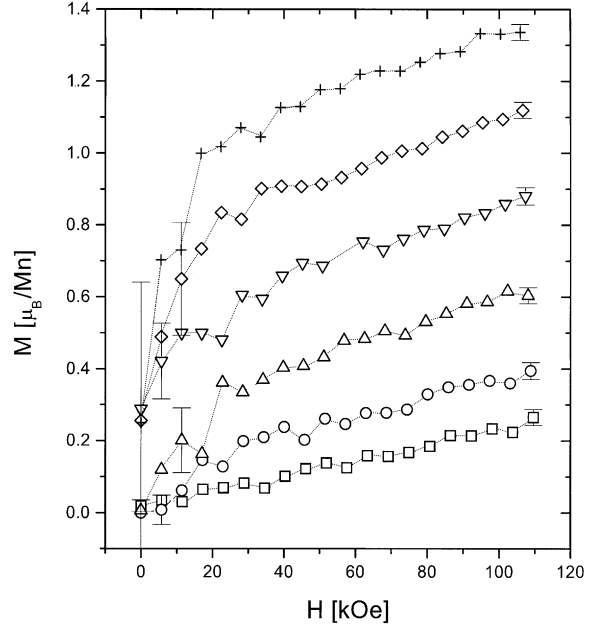


Fig. 3. Magnetization M vs. H for $x=0$ (squares), $\frac{1}{48}$ (circles), ..., $\frac{5}{48}$ (plus signs), obtained by MC calculations. Characteristics error bars are displayed for few points.

model considered, there is a competence between AF–SE and FM–DE interactions. Preliminary calculations [4] show that a polaronic phase is obtained for $K/t \geq 0.6x$. These polarons are immersed in the otherwise AF background. As we apply a magnetic field, the FM polarons tend to align in the direction of H . We calculated $M(T, x, H)$ averaging over 5000 MC realizations and sites. M_0 was obtained extrapolating a linear dependence from the highest fields ($40 \text{ kOe} \leq H \leq 120 \text{ kOe}$). When all polarons are aligned, the ratio M_0/x gives a measurement of the polaron size. The high field differential slope of M vs. H calculated in this case would then arise from two main processes: enlargement of the polarons and canting of the AF background.

The slope at high fields is of the same order in all the samples. The linear response in the case $x = 0$, is due only to the canting of the AF background, $\chi(x = 0) \propto K^{-1}$. For $x > 0$, in the range $H \leq 75$ kOe, we find a rapid growth of M vs. H , although strong fluctuations are present due to finite-size effects. In this regime the polarons,

originally randomly oriented, start to align with H [1]. The numerical results suggests that full alignment is not completely reached at 50 kOe, which is our experimental limit.

In Fig. 2(a), we compare the M_0 vs. x dependence obtained numerically, with the experimental values at 5 K. As we mentioned above, the slope of M_0 vs. x is a measurement of the magnetic moment of the polaron created by each e_g electron added. In the experiments, we find for $x < 0.03$, that each polaron has a magnetic moment of $1\mu_B$, and for $x > 0.03$, increases up to $7\mu_B/\text{polaron}$. In the present model, we find a linear dependence in the curve M_0 vs. x . The size of each polaron is fixed by the ratio K/t [4]. The distribution of the itinerant charge, shows that each polaron extends over 5–6 sites. The differential susceptibility χ is a measurement of the canting of the AF background and the enlargement of polarons with H . In Fig. 2(b) we show the calculated χ vs. x , that shows an almost constant behavior. Since for $x = 0.1$, about half of the sites take part in the polaron phase, we conclude that the response of polarons to H is of the same order to that of the canting of the AF background.

We found a remarkable agreement between experimental and numerical values of M_0 and χ . The numerical simulations suggest that linear

regime M vs. H , is not fully reached at $H = 50$ kOe, thus experiments at higher fields are suggested in order to make a better comparison with numerical prediction, specially in the low-doped regime, where some discrepancies are observed.

Acknowledgements

We acknowledge partial support from AN-PCYT (Argentina)-PICT 3-52-1027/3-05266, and CONICET(Argentina)-PIP 4947/96. H.A. is CONICET (Argentina) PhD-fellow.

References

- [1] H. Aliaga, B. Alascio, M.T. Causa, H. Salva, G. Leiva, G. Polla, P. Perazzo, D. Vega, A. Butera, preprint cond-mat/0010295.
- [2] H. Aliaga, M.T. Causa, B. Alascio, H. Salva, M. Tovar, D. Vega, G. Polla, G. Leyva, P. Konig, J. Magn. Magn. Mater. 226–230 (2001) 791.
- [3] D. Vega, G. Polla, A.G. Leyva, P. Konig, H. Lanza, A. Esteban, H. Aliaga, M.T. Causa, M. Tovar, B. Alascio, J. Solid State Chem. 156 (2001) 458.
- [4] H. Aliaga, unpublished.